Supplementary Information for

Infrared micro-detectors with high sensitivity and high response speed using VO_2-coated helical carbon nanocoils

He Ma, [a] Xinping Zhang,*[a] Zhichao Zhang,[b] Yu Wang,[a] Guang Wang,[c] Feifei Liu,[d] Ruixue Cui,[e] Cuiying Huang,[a] Meng Wang,[a] Yang Wei,[c] Kaili Jiang,[c] Lujun Pan*[e] and Kai Liu*[b]

a. College of Applied Sciences, Beijing University of Technology, Beijing 100124, P. R. China.
b. State Key Laboratory of New Ceramics and Fine Processing, School of Materials Science and Engineering, Tsinghua University, Beijing 100084, P. R. China.
c. State Key Laboratory of Low-Dimensional Quantum Physics, Tsinghua-Foxconn Nanotechnology Research Center, Department of Physics, Collaborative Innovation Center of Quantum Matter, Tsinghua University, Beijing 100084, P. R. China
d. Department of Physics, Fudan University, 220 Handan Rd., Yangpu District, Shanghai 200433, P. R. China
e .School of Physics and Optoelectronic Technology, Dalian University of Technology, No. 2 Linggong Road, Ganjingzi District, Dalian 116024, P. R. China.

1. Thermal transfer model for the CNC under infrared light irradiation

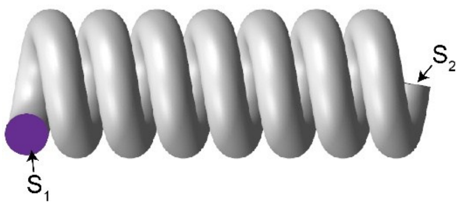

Figure S1. Geometrical model of a CNC in the thermal transfer model.

In the 3D steady-state thermal transfer equation $\nabla\cdot(-k\nabla T)=Q$, k is the thermal conductivity of CNC. The thermal conductivity of the individual CNC was 5 W/(m·k). The thermal source (Q, W/m^3) corresponded to the thermal energy absorbed from the infrared irradiation by the CNC. In our model, Q was calculated by $((P\times S)/V)\times A$, where P was the power density of infrared irradiation, S was the projection area of the CNC, V was the volume of the CNC and A is the absorbance of the CNC. P and A were set to be 1 mW/mm^2 and 100%, respectively. Because surfaces S_1 and S_2 were connected to the substrate, the boundary conditions for them (Figure S1) were $T_{s1} = T_{s2}$ =298 K. For other surface, the adiabatic boundary condition-$n\cdot\nabla(-k\nabla T)=0$, was adapted due to the vacuum environment. The simulation was performed by the COMSOL Multiphysics software.

2. Preparation processes of a VO_2/CNC bolometer

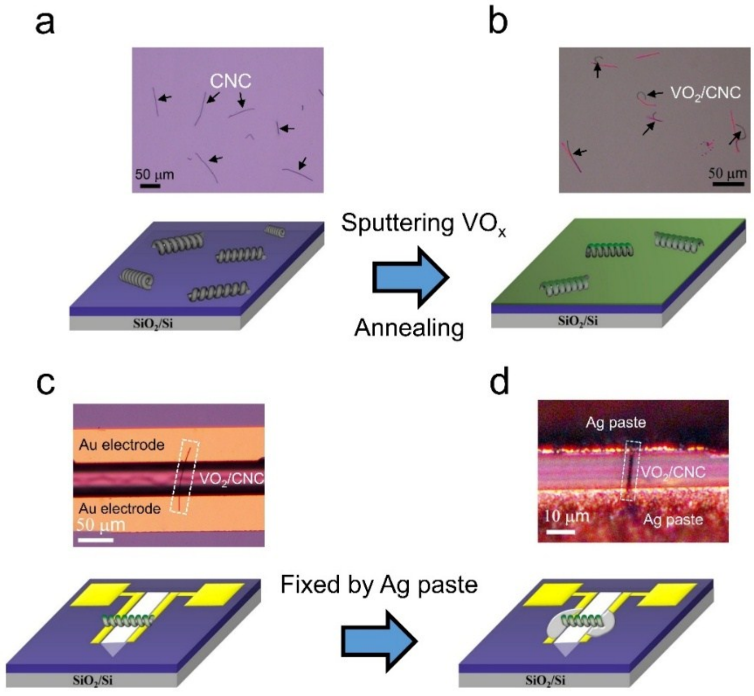

Figure S2. Schematic of fabrication processes of a VO_2/CNC bolometer. (a) Transferring individual CNCs from as-grown CNC powders to a SiO_2 substrate. (b) Sputtering VO_x on the CNC and then annealing. (c) Transferring the VO_2/CNC to the patterned substrate. (d) Fixed the VO_2/CNC on the Au electrodes by Ag paste.

3. Scanning electron microscopy characteristic of VO_2/CNC bolometer

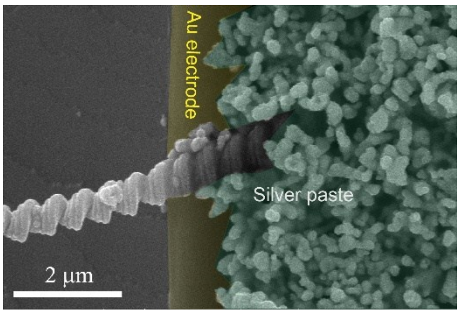

Figure S3. Enlarged scanning electron microscope (SEM) image of the contact between the VO_2/CNC and the Au electrode.

4. Scanning electron microscopy characteristic of a pristine CNC

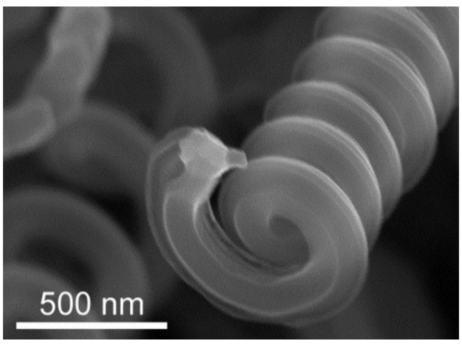

Figure S4. SEM image of a pristine CNC.

5. V_{out} of the VO_2/CNC bolometer under different light power

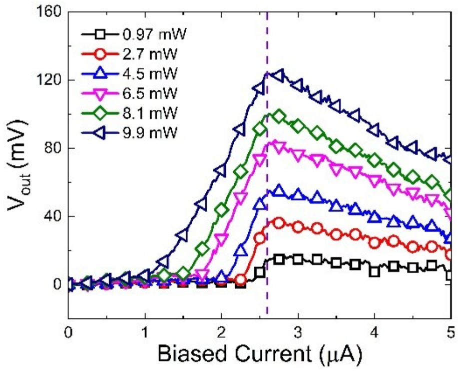

Figure S5. V_{out} of the VO_2/CNC bolometer under various biased current and different light power.

6. Simulation of temperature distribution of the CNC induced by joule heating

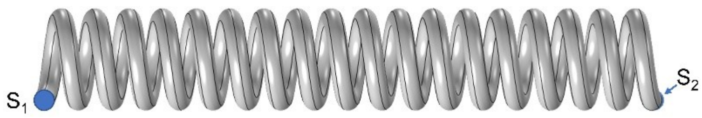

Figure S6. Geometrical model of a CNC in the simulation.

We simulated the temperature distribution of a CNC at different biased current by the coupling of the heat transfer module and the AC/DC module in COMSOL Multiphysics software. In the simulation, the thermal conductivity of the individual CNC was 5 W/(m·k). The fiber diameter, coil diameter, pitch and length of the CNC used in the simulation were 300 nm, 1200 nm, 500 nm and 9 μm, respectively. The resistivity of the CNC was 2.1×10^{-4} Ω·m.[1] As shown in Figure S6, in the heat transfer module, because surfaces S_1 and S_2 were connected to the substrate, the boundary conditions for them were $T_{s1} = T_{s2}$ =298 K. For other surface, the adiabatic boundary condition-$n\cdot\nabla(-k\nabla T)=0$, was adapted due to the vacuum environment. In the boundary conditions for the AC/DC module, the electrical potential of S_1 was set to a desired value and the electrical potential of S_2 was fixed at zero. The current flowing along the CNC was calculated by V_{S1}/R_{cnc}.

As shown in Figure S7a, due to joule heating by the current of 9.4 μA, the temperature maximized (341 K) at the center and decreased along the axis of the CNC to both ends. Therefore, this temperature distribution of the CNC induced by joule heating could just stimulate phase transition of VO_2 around the center of the CNC. Considering the ΔT was maximum around the center of the CNC under infrared irradiation (Figure 1b), the voltage output of VO_2/CNC would become maximum at the optimum current, which was 9.4 μA in the case of this simulation. With the increase of the biased current to 11 μA, the CNC was heated beyond the MIT temperature around the center, which changed VO_2 around the center of the CNC to metallic state completely. However, around both ends, the temperature of VO_2/CNC was still lower than the MIT temperature because of the thermal dissipation, and thereby VO_2 stayed insulator phases around both ends. Further increase of the biased current would elongate the length of metallic phase and shorten that of insulator phases. Even though a part of VO_2 on the CNC still work at MIT temperature, the corresponding ΔT around both ends of the CNC induced by the infrared irradiation was smaller than the ΔT around the center of the CNC, which leading to the decrease of the voltage output.

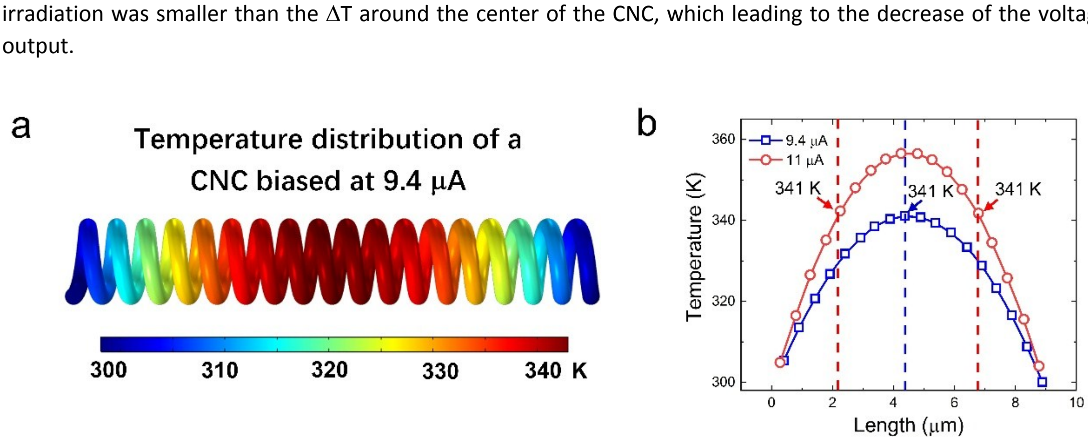

Figure S7. (a) Simulated temperature distribution of a CNC at 9.4 μA. (b) Comparison of temperature along the CNC surface at 9.4 μA and 11 μA.

7. Infrared response of VO_2/CNC bolometer in air

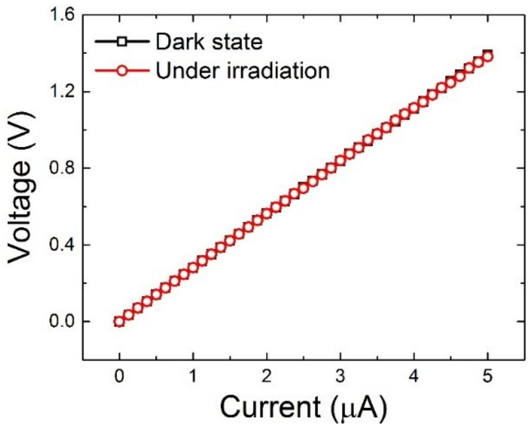

Figure S8. I-V curves of the VO_2/CNC in air under dark state and under infrared light irradiation with a power of 6.5 mW at 808 nm.

8. Simulation of the absorbance of a pristine CNC

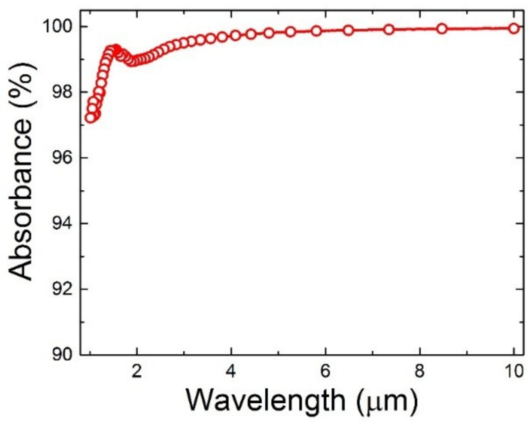

Figure S9. Simulated absorbance of a CNC in the wavelength from 1 to 10 μm.

The simulation for the absorbance of the CNC was performed by the Lumerical software. In the simulation, a circularly polarized Gaussian beam with wavelengths from 1 to 10 μm was irradiated on the CNC. The waist radius of the Gaussian beam was set as 6 μm. The fiber diameter, coil diameter, pitch and length of the CNC were set as 500 nm, 1000 nm, 600 nm and 1200 nm, respectively. The optical constant of CNC was the same as the amorphous graphite because of the similarity in crystal structure between the CNC and the amorphous graphite. The optical constant of amorphous graphite was obtained from the material database of Comsol Multiphysics software and was imported into Lumerical software for simulation. We simulated the transmission (T) and reflection of the CNC (R) and then the absorbance of the CNC was calculated by the equation 1-T-R.

Reference

1. H. Ma, K. Nakata, L. J. Pan, K. Hirahara and Y. Nakayama, *Carbon*, 2014, **73**, 71-77.